

Indeterminacy, Memory, and Motion in a Simple Granular Packing

Sean McNamara,* Ramón García-Rojo, and Hans Herrmann
Institut für Computerphysik, Universität Stuttgart, 70569 Stuttgart, GERMANY

(Dated: November 7, 2018)

We apply two theoretical and two numerical methods to the problem of a disk placed in a groove and subjected to gravity and a torque. Methods assuming rigid particles are indeterminate – certain combinations of forces cannot be calculated, but only constrained by inequalities. In methods assuming deformable particles, these combinations of forces are determined by the history of the packing. Thus indeterminacy in rigid particles becomes memory in deformable ones. Furthermore, the torque needed to rotate the particle was calculated. Two different paths to motion were identified. In the first, contact forces change slowly, and the indeterminacy decreases continuously to zero, and vanishes precisely at the onset of motion, and the torque needed to rotate the disk is independent of method and packing history. In the second way, this torque depends on method and on the history of the packing, and the forces jump discontinuously at the onset of motion.

PACS numbers: 45.70.-n

I. INTRODUCTION

A. Motivation

Static granular packings present many difficulties to theorists seeking to understand them. One complication is *indeterminacy*. If the grains are assumed to be perfectly rigid but with friction, one cannot find a unique solution for the forces between them; there are usually many possible solutions [1, 2, 3, 4, 5]. If one calculates forces from particle displacements, indeterminacy disappears, but in many examples, these displacements are tiny fractions of a grain diameter. It is astonishing that such tiny distances would change the fundamental nature of the problem. Furthermore, it is not clear how the unique state, determined by particle displacements, is related to the set of possible forces arising when the particles are rigid. These questions are made more pressing by the widespread use of simulation methods that assume the particles are rigid, and hence somehow choose one value for the contact forces out of many possible solutions.

Next, there is the question of *memory*. The method of construction of a packing and its history change its behavior. For example, it has been shown that the method of construction changes the distribution of forces under a sand pile [6, 7, 8]. In this case, the memory of the packing seems to be stored in the orientation of the contacts [8].

Finally, there is the onset of *motion*: what forces are needed to permanently deform a static packing, and how does this motion originate? These questions are the principal concern of soil mechanics. Motion often is very localized, i.e., in shear bands [9, 10]. Another phenomena related to the onset of motion is the linear accumulation of deformation in granular assemblies subjected to

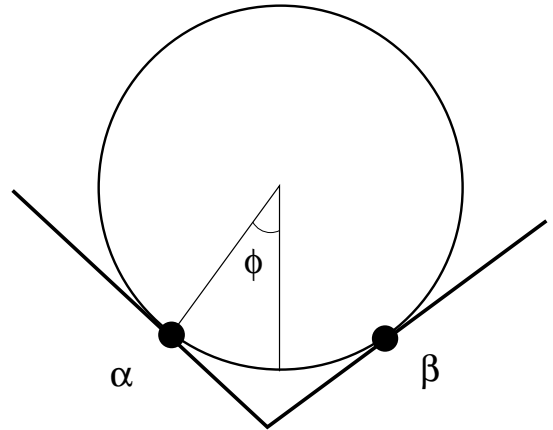


FIG. 1: A disk supported by two walls through contacts α and β . The angle ϕ suffices to characterize the geometry.

periodically varying forces [11, 12].

In this paper, we consider a very simple system where the relationships between these problems is clearly demonstrated. We hope that it will provide clues on how to understand much more complicated packings.

B. Synopsis

The granular “packing” shown in Fig. 1 is perhaps the simplest possible granular packing. Nevertheless, it exhibits many subtleties, and in this paper we use it as an example to show the relationship between indeterminacy, memory, and motion. This configuration is similar to the rod wedged between two converging walls discussed in Ref. [5]. It is even simpler than the one considered in Ref. [13], where a disk is placed in an asymmetric groove and subjected to gravity. Here, we consider only a symmetric groove, but the forces we impose on the disk are more complicated. In addition to a gravitational acceleration g , we apply a torque $\tau > 0$. The contacts between

*Email address: sean@ica1.uni-stuttgart.de

the disk and the wall are assumed to be non-cohesive and frictional, with Coulomb friction ratio μ . We investigate two questions: How do the contact forces at α and β change in response to the imposed forces? At what value of the torque does the particle begin to rotate?

We first examine some general considerations: the equations of static equilibrium, and the status of the contacts. Then we attempt to deduce the contact forces from these considerations. We show that for certain geometries and torques, one cannot decide whether the disk rotates or not. We then present a series of contact dynamics (hereafter CD) [14] and molecular dynamics (hereafter MD) [15] simulations, and point out the difference between them. Then we formulate a second method of calculating the contact forces, assuming they arise from small deformations of the particles. This second method explains all the features of the MD simulations, and sheds light on the questions mentioned above.

II. RIGID PARTICLES

A. Static Equilibrium

The equations of static equilibrium for the disk in Fig. 1 are

$$\begin{aligned} R_\alpha \sin \phi + T_\alpha \cos \phi - R_\beta \sin \phi + T_\beta \cos \phi &= 0, \\ R_\alpha \cos \phi - T_\alpha \sin \phi + R_\beta \cos \phi + T_\beta \sin \phi &= mg, \\ rT_\alpha + rT_\beta &= -\tau. \end{aligned} \quad (1)$$

Here, R_α indicates the normal force at contact α , with $R_\alpha > 0$ for repulsion. T_α is the tangential force, with $T_\alpha > 0$ when this force exerts a positive torque on the disk. R_β and T_β are defined in the same way.

These equations can be written in matrix form:

$$\mathbf{c}\mathbf{F} + \mathbf{f}_{\text{ext}} = 0. \quad (2)$$

We call \mathbf{c} the *contact matrix*:

$$\mathbf{c} = \begin{pmatrix} \sin \phi & \cos \phi & -\sin \phi & \cos \phi \\ \cos \phi & -\sin \phi & \cos \phi & \sin \phi \\ 0 & r & 0 & r \end{pmatrix}. \quad (3)$$

Note that the dimensions of \mathbf{c} require that it have at least one null eigenvalue. The contact forces \mathbf{F} and the external forces \mathbf{f}_{ext} are

$$\mathbf{F} = \begin{pmatrix} R_\alpha \\ T_\alpha \\ R_\beta \\ T_\beta \end{pmatrix}, \quad \mathbf{f}_{\text{ext}} = \begin{pmatrix} 0 \\ -mg \\ \tau \end{pmatrix}, \quad (4)$$

where R_α (R_β) are the normal components forces exerted at contact α (β), and T_α and T_β are the tangential components.

It is convenient to use the following orthogonal basis of \mathbb{R}^4 :

$$\begin{aligned} \mathbf{F}_x &= \frac{1}{2} \begin{pmatrix} \sin \phi \\ \cos \phi \\ -\sin \phi \\ \cos \phi \end{pmatrix}, & \mathbf{F}_y &= \frac{1}{2} \begin{pmatrix} \cos \phi \\ -\sin \phi \\ \cos \phi \\ \sin \phi \end{pmatrix}, \\ \mathbf{F}_\theta &= \frac{1}{2} \begin{pmatrix} -\cos \phi \\ \sin \phi \\ \cos \phi \\ \sin \phi \end{pmatrix}, & \mathbf{F}_0 &= \frac{1}{2} \begin{pmatrix} \sin \phi \\ \cos \phi \\ \sin \phi \\ -\cos \phi \end{pmatrix}. \end{aligned} \quad (5)$$

If \mathbf{F} is written in this basis:

$$\mathbf{F} = a_x \mathbf{F}_x + a_y \mathbf{F}_y + a_\theta \mathbf{F}_\theta + a_0 \mathbf{F}_0, \quad (6)$$

then one can verify that

$$\mathbf{c}\mathbf{F} = \begin{pmatrix} a_x \\ a_y \\ a_x r \cos \phi + a_\theta r \sin \phi \end{pmatrix} = -\mathbf{f}_{\text{ext}}. \quad (7)$$

This equation enables one to easily construct solutions to Eq. (2), for one has immediately $a_x = 0$, $a_y = mg$, and $a_\theta = -\tau/(r \sin \phi)$. However, a_0 cannot be determined in this way because \mathbf{F}_0 is a null eigenvector of \mathbf{c} . This is an expression of the indeterminacy in the problem.

B. Contact Status

Of course, one does not have absolute freedom to choose a_0 , because the following conditions must be satisfied at the contacts:

$$R \geq 0, \quad \mu R \geq |T|, \quad (8)$$

where the constant μ is the Coulomb friction ratio. The first inequality excludes cohesive forces, and the second requires that the tangential forces not exceed a certain threshold.

At this point, it is useful to introduce the concept of contact *status*. If we have equality in the second condition in Eq. (8), the contact is said to be *sliding*, otherwise it is *non-sliding*. The tangential relative motion v_t must be consistent with the contact status. If the contact is non-sliding, no tangential motion is allowed, but if the contact is sliding, then the tangential force must oppose the motion. Note that $v_t = 0$ is allowed under all circumstances, so that contacts in static equilibrium can be sliding.

To see how this limits the possible values of a_0 , one can first use the definition of \mathbf{F} in Eq. (4) and the basis in Eq. (5) to compute the forces in terms of μ , ϕ , and the coefficients in the expansion of Eq. (6). Then one can use Eq. (7) to eliminate all the coefficients except for a_0 . Finally, one forms the inequalities $\mu R_\alpha \geq -T_\alpha$,

$\mu R_\alpha \geq T_\alpha$, $\mu R_\beta \geq -T_\beta$, and $\mu R_\beta \geq T_\beta$. These yield

$$a_0 (\mu \tan \phi + 1) + \left[mg + \frac{\tau}{r \sin \phi} \right] (\mu - \tan \phi) \geq 0, \quad (9a)$$

$$a_0 (\mu \tan \phi - 1) + \left[mg + \frac{\tau}{r \sin \phi} \right] (\mu + \tan \phi) \geq 0, \quad (9b)$$

$$a_0 (\mu \tan \phi - 1) + \left[mg - \frac{\tau}{r \sin \phi} \right] (\mu + \tan \phi) \geq 0, \quad (9c)$$

$$a_0 (\mu \tan \phi + 1) + \left[mg - \frac{\tau}{r \sin \phi} \right] (\mu - \tan \phi) \geq 0, \quad (9d)$$

Some of these conditions are redundant. For example, Eq. (9c) implies Eq. (9b). To see this, note that due to our choice $\tau > 0$,

$$\left[\frac{2\tau}{r \sin \phi} \right] (\mu + \tan \phi) \geq 0. \quad (10)$$

Adding this to Eq. (9c) gives Eq. (9b). Thus Eq. (9b) never needs to be considered; it will be satisfied as long as Eq. (9c) is. Similar reasoning can be used to show that Eq. (9a) is redundant when $\mu - \tan \phi > 0$, and that Eq. (9d) is redundant when $\mu - \tan \phi < 0$. When $\mu = \tan \phi$, these conditions are equivalent.

The conditions in Eqs. (9) put limits on the value that a_0 can attain [4]. Furthermore, when a contact is sliding, we have equality in one of the above cases, and a_0 is determined: indeterminacy disappears.

C. Application

We now attempt to deduce the contact forces and particle motion, using only the considerations presented above. No relation between particle deformation and contact forces is assumed. Note that the biggest difficulty will be determining the coefficient a_0 ; the other three coefficients in the expansion in Eq. (6) can be read off from Eq. (7). The unknown value of a_0 is an expression of the indeterminacy of the problem. We must consider three separate cases, depending on the relation of μ to the slope of the sides of the groove, $\tan \phi$.

1. Shallow slope: $\tan \phi < \mu$

Let us first restrict ourselves to $\tan \phi < \mu$ and $\mu < 1$. Under these assumptions, we have $\mu - \tan \phi > 0$, so the a_0 is constrained by the conditions Eqs. (9c) and (9d). Furthermore, $\mu \tan \phi - 1 < 0$, so that Eq. (9c) sets a lower, and Eq. (9d) an upper bound on a_0 :

$$a_{\min} \leq a_0 \leq a_{\max}, \quad (11)$$

where

$$a_{\min} = - \left[mg - \frac{\tau}{r \sin \phi} \right] \left(\frac{\mu - \tan \phi}{1 + \mu \tan \phi} \right),$$

$$a_{\max} = \left[mg - \frac{\tau}{r \sin \phi} \right] \left(\frac{\mu + \tan \phi}{1 - \mu \tan \phi} \right). \quad (12)$$

The quantities in the curved brackets are always positive, while the quantity in the square brackets is positive for $\tau = 0$, and decreases as τ increases. It vanishes when

$$\tau = \tau_1 \equiv mgr \sin \phi, \quad (13)$$

and becomes negative when $\tau > \tau_1$. When it is negative, no solution for a_0 exists, for $a_{\min} > a_{\max}$. Thus there are no solutions of the equations of static equilibrium, when $\tau > \tau_1$ that also satisfy Eq. (8), and the disk must move. On the other hand, when $\tau < \tau_1$, an infinite number of such solutions exist, one for each value of a_0 satisfying Eq. (11). Finally, at $\tau = \tau_1$, we have $a_{\min} = a_0 = a_{\max} = 0$, hence there is a unique solution.

We have shown that the disk must rotate when $\tau > \tau_1$, and that static solutions exist for $\tau \leq \tau_1$, but we have not yet shown that the disk will not move when $\tau \leq \tau_1$. After all, for some choice of a_0 , it might be possible to put the disk in motion. But this can be shown to be impossible by considering what happens at $\tau = \tau_1$. In this situation, we have $a_0 = 0$, so the contact forces are

$$R_\alpha = mg \cos \phi, \quad T_\alpha = -mg \sin \phi, \quad R_\beta = T_\beta = 0. \quad (14)$$

Thus the disk is entirely supported by contact α . R_α and T_α cancel the gravitational force, and τ balances the torque $rT_\alpha = -\tau_1$ exerted on the disk by the contact force. A small increase in τ and T_α will cause the disk to roll upwards to the left, out of the groove. On the other hand, if $\tau < \tau_1$, then the torque $rT_\alpha = -\tau_1$ will not be balanced, and the disk will try to roll down the slope. Therefore, if $\tau < \tau_1$, the disk cannot rotate.

Another possibility is that the disk rotate in place. But this is impossible, when $\tan \phi < \mu$, because this requires $T_\alpha = -\mu R_\alpha$ and $T_\beta = -\mu R_\beta$, i.e., contacts α and β must be sliding. This occurs when we have equality in both Eqs. (9a) and (9c). But this cannot happen because when equality holds in Eq. (9a), then Eq. (9d) is violated.

Therefore, the value of a_0 has no effect on the motion of the disk. If $\tau < \tau_1$, the disk remains in the groove, although the forces cannot be uniquely determined. At $\tau = \tau_1$, there is a unique solution for the forces: contact β opens and the particle's weight is supported by contact α . For $\tau > \tau_1$, the disk rolls out of the groove.

Note that there is a relationship between the onset of motion and the disappearance of indeterminacy: we have motion for $\tau > \tau_1$ and indeterminacy for $\tau < \tau_1$. Indeed, we could have anticipated this when we wrote down Eqs. (9). For a disk to move, at least one contact must be sliding (or open), leading to an equality in at least one of Eqs. (9). Then this equality can be used to determine a_0 , eliminating the indeterminacy.

2. *Intermediate slope: $\mu < \tan \phi < 1/\mu$*

Now let us consider intermediate angles $\mu \leq \tan \phi \leq 1/\mu$. At these values of ϕ , the relevant conditions from Eqs. (9) are Eqs. (9a) and (9c). Eq. (9c) sets an upper, and Eq. (9a) a lower, bound on a_0 . Thus we have Eq. (11) again, except now

$$\begin{aligned} a_{\min} &= \left[mg + \frac{\tau}{r \sin \phi} \right] \left(\frac{\tan \phi - \mu}{1 + \mu \tan \phi} \right), \\ a_{\max} &= \left[mg - \frac{\tau}{r \sin \phi} \right] \left(\frac{\tan \phi + \mu}{1 - \mu \tan \phi} \right). \end{aligned} \quad (15)$$

Again, the quantities in the curved brackets is positive for $\mu < \tan \phi < 1/\mu$. The quantities in the square brackets are equal and positive for $\tau = 0$. But as τ increases, a_{\min} increases while a_{\max} decreases. When

$$\tau = \tau_2 \equiv mgr \frac{\mu}{1 + \mu^2} \sec \phi, \quad (16)$$

we have $a_{\min} = a_0 = a_{\max} = a_2$, where

$$a_2 = mg \left[1 + \frac{\mu}{\tan \phi} \frac{1 + \tan^2 \phi}{1 + \mu^2} \right] \left(\frac{\tan \phi - \mu}{1 + \mu \tan \phi} \right). \quad (17)$$

and there is a unique solution for the contact forces. When $\tau > \tau_2$, no static solution satisfying the contact conditions exists, as $a_{\min} > a_{\max}$.

Furthermore, we can show that the disk cannot move when $\tau < \tau_2$. The disk cannot roll out of the groove, because the forces in Eq. (14) violate $|T_\alpha| \leq \mu R_\alpha$. If the disk is to rotate in place, we must have $T_\alpha = -\mu R_\alpha$ and $T_\beta = -\mu R_\beta$, i.e., we must have equality in Eqs. (9a) and (9c). But we have just showed that requiring these equalities leads to $\tau = \tau_2$, $a_{\min} = a_0 = a_{\max}$.

Therefore, we have exactly the same situation as in Sec. II C 1. For $\tau < \tau_2$, there is indeterminacy without motion, and for $\tau > \tau_2$ there is motion. There is a unique solution for the forces precisely at $\tau = \tau_2$. Furthermore, note that $\tau_1 = \tau_2$ when $\tan \phi = \mu$ and when $\tan \phi = 1/\mu$.

3. *Large slopes: $\tan \phi > 1/\mu$*

At large angles ($\tan \phi > 1/\mu$), the relevant conditions are still Eqs. (9a) and (9c) as in the previous section. But now the factor $1 - \mu \tan \phi$ becomes negative, transforming Eq. (9c) into a *lower* bound on a_0 . Eq. (9a) remains a lower bound on a_0 , meaning that there is no upper bound on a_0 . It can be made arbitrarily large. Therefore, for any $\tau > 0$, it is possible to satisfy all conditions in Eq. (9) simply by making a_0 very large. (Note that all the factors multiplying a_0 in these conditions are positive when $\tan \phi > 1/\mu$). This means that an infinite torque can be put on the disk without causing it to rotate.

On the other hand, if $\tau = \tau_2$, one can obtain equality in Eqs. (9a) and (9c), meaning contacts α and β are sliding. If τ is increased slightly, then the disk can start to rotate

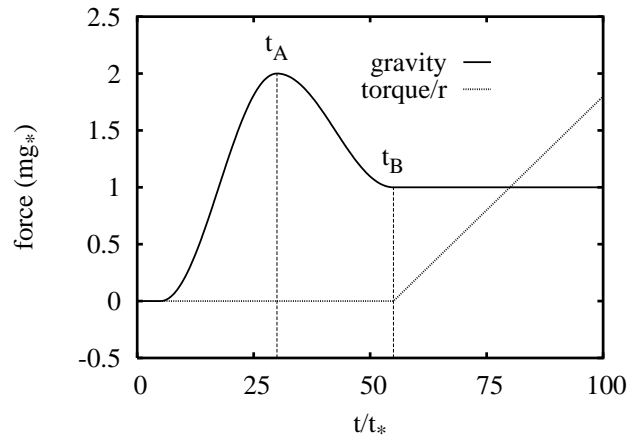


FIG. 2: The forces applied to the disk. Time is given in units of $t_* = \sqrt{d/g}$. The gravity attains a maximum at $t = t_A$, and the torque begins to increase at $t = t_B$.

in place. Therefore, both static and moving solutions co-exist for $\tau > \tau_2$, and we cannot decide on the basis of Eqs. (9) whether the disk rotates or not.

This remarkable situation poses two questions: First, how will the CD algorithm handle this case? This algorithm tries to use the information presented in Sec. II to deduce the motion of the particles, but we have shown that this is insufficient. Secondly, it would be very easy to construct an experiment to measure the torque needed to make the disk rotate. One could construct a groove with $\tan \phi > 1/\mu$, and place a cylinder in the groove, and try to turn the cylinder. What determines whether the cylinder rotate? These questions are investigated in the next sections.

III. SIMULATIONS

To verify the conclusions of the previous section, and to clarify the situation for $\tan \phi > 1/\mu$, we carried out CD and MD simulations. The disk was placed in the groove without any forces acting on it. Then gravity was turned on, and increased, until it reached a maximum of g_{\max} at $t = t_A$. Then it was decreased, reaching g_* at $t = t_B$, and thereafter was held constant. A linearly increasing torque τ was then applied until the particle began to rotate. Fig. 2 shows the gravity force and torque as functions of time. In the following, we will vary g_{\max} , but keep g_* fixed. In all cases, $\mu = 0.5$.

The experiment can be considered as a very simple soil mechanics experiment. First, the sample, consisting of one disk, is “prepared” by pushing the disk into the groove, and “loaded” by the torque until it “yields”. We are especially interested in knowing if and how the preparation affects the yielding torque.

A typical result of a simulation is shown in Fig. 3. The three non-zero coefficients a_y , a_θ , and a_0 of the expansion

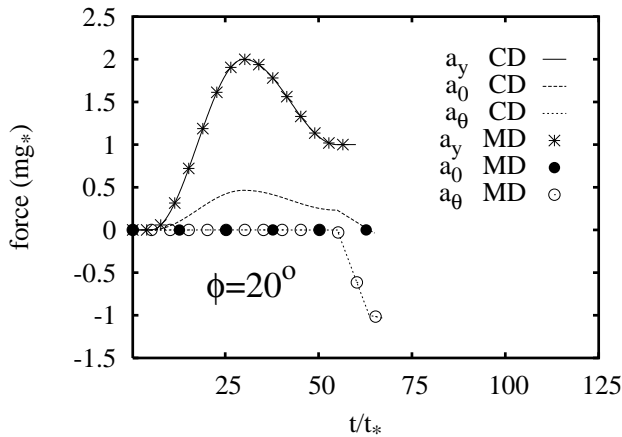


FIG. 3: The coefficients of the expansion, Eq. (6), as a function of time. Here $\phi = 20^\circ$ and $\mu = 0.5$ so that $\tan \phi < \mu$. The curves stop when the particle begins to rotate.

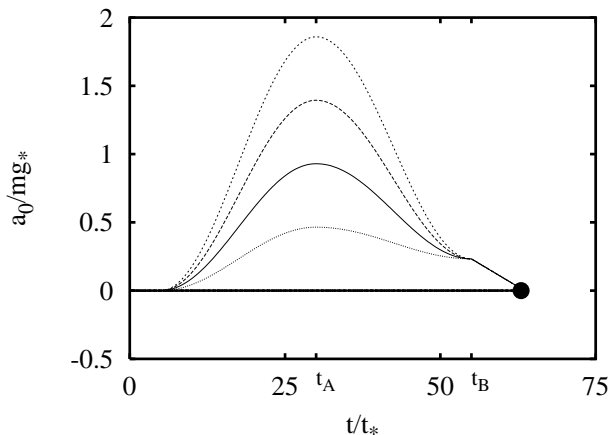


FIG. 4: The coefficient a_0 as a function of time for various values of g_{\max}/g_* . Here $\phi = 20^\circ$ and $\mu = 0.5$, so that $\tan \phi < \mu$. The thin lines are the CD simulations, with $g_{\max}/g = 2$ (lowest curve), 4, 6, and 8 (highest curve). The thick lines are the corresponding MD simulations, which fall on top of each other in this case. The large dot indicates the point where the disk begins to rotate.

in Eq. (6) are shown. In accordance with Eq. (7), a_y and a_θ are identical for the CD and MD solution methods, and given by $a_y = mg$, $a_\theta = -\tau/(r \sin \phi)$. The coefficient a_0 , however, differs between the CD and MD solutions. In the following, we will plot only a_0 , as the other coefficients are always uniquely determined by the imposed forces. Three different values of ϕ will be considered, corresponding to the three subsections of Sec. II C.

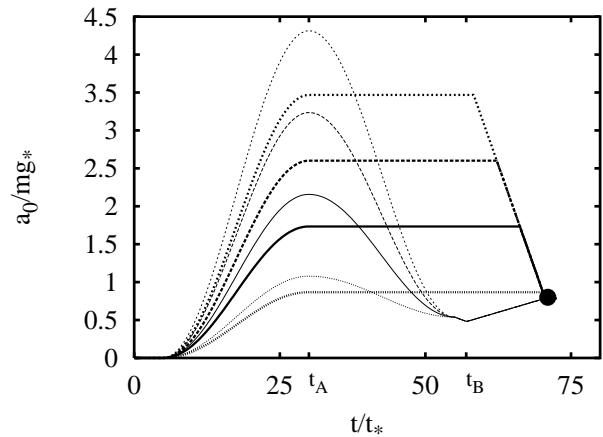


FIG. 5: The undetermined coefficient a_0 from Eq. (6) as a function of time. Here, $\phi = 50^\circ$ and $\mu = 0.5$, so that $\mu < \tan \phi < 1/\mu$. The thin lines are the CD simulations, with $g_{\max}/g = 2$ (lowest curve), 4, 6, and 8 (highest curve). The thick lines are the MD simulations with the same values of g_{\max}/g . The large dot indicates the point where the disk begins to rotate.

A. Shallow Slopes: $\tan \phi < \mu$.

In Fig. 4, we plot a_0 as a function of time for the MD and CD simulations. In the MD simulations, $a_0 = 0$, independent of time and of g_{\max} . In the CD simulation, a_0 is proportional to the gravity for $t < t_B$. Note that the values of a_0 are significant – almost twice the weight of the particle for $g_{\max}/g_* = 8$. However, at $t = t_B$, all CD simulations have the same value of a_0 . As the torque is applied, a_0 moves linearly towards 0. This occurs because when $\tau \leq \tau_1$, the disk cannot move, but a_0 is constrained between the two values given in Eq. (12), which approach each other as τ approaches τ_1 . Indeed, the diagonal line segment near $50 < t/t_* < 60$ traced out by the CD simulations corresponds to requiring equality in Eq. (9d). The conditions Eqs. (9c) and (9d) act as a “funnel” that guides a_0 toward 0 as the torque increases, so that $a_0 = 0$ when $\tau = \tau_1$. Thus the MD and CD both predict that the disk moves at $\tau = \tau_1$. However, the two methods predict different routes to failure. MD predicts that both contacts remain non-sliding until the force at β vanishes, and the disk starts to roll. On the other hand, CD predicts that the contact at β first becomes sliding, and then later starts to roll.

B. Intermediate Slopes: $\mu < \tan \phi < 1/\mu$.

In Fig. 5, we show a_0 for the case of intermediate slope $\mu < \tan \phi < 1/\mu$. The behavior of the CD simulation is quite similar to the preceding case. For $t < t_B$, a_0 is again proportional to gravity, but attaining even larger values than before. At $t = t_B$, all CD simulations are identical,

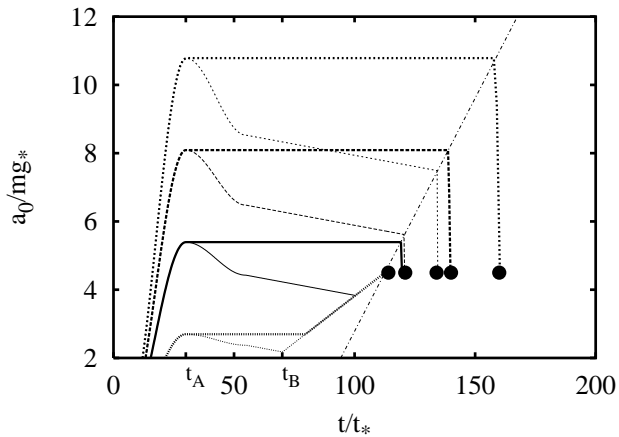


FIG. 6: Coefficients of the expansion Eq. (6) as a function of time. Here, $\phi = 80^\circ$ and $\mu = 0.5$, so that $\tan \phi > 1/\mu$. The thin lines are the CD simulations, with $g_{\max}/g = 2$ (lowest curve), 4, 6, and 8 (highest curve). The thick lines are the MD simulations with the same values of g_{\max}/g . The dots indicate the points where the disk begins to rotate. The diagonal dot-dashed line is obtained by requiring equality in Eq. (9c).

and they evolve together during the loading. They again encounter the “funnel” arising from the lower and upper bounds on a_0 given in Eq. (15), and move toward $a_0 = a_2$, and the disk starts to rotate when $\tau = \tau_2$.

The MD simulation has a quite different behavior. For $t < t_A$, a_0 is also proportional to the gravity, although lower than the CD value. But for $t > t_A$, a_0 remains constant, so that a_0 is proportional to g_{\max} , even at $t = t_B$. In this case, therefore, the preparation does make a difference. The MD simulations remember the value of g_{\max} , and this memory is stored in a_0 . This simple example clearly demonstrates a principle stated in the paper’s introduction: the indeterminacy of forces in perfectly rigid particles is related to history-dependency in packings of deformable particles. The coefficient a_0 , which is undetermined in the perfectly rigid case, here contains the memory of the packing, and is simply proportional to the greatest downward force that the disk has experienced in the past.

The history dependency of the MD simulation, however, does not affect the yielding torque. The different MD simulations encounter the funnel at different times, but are all guided towards the point $\tau = \tau_2$, $a_0 = a_2$, where the disk begins to rotate. Therefore, the memory on the MD simulation can only be detected by inspecting the contact forces.

C. Large Slopes: $\tan \phi > 1/\mu$.

Finally, in Fig. 6, we show the case where $\tan \phi > 1/\mu$. This case has some important differences from the

preceding cases. First of all, both the CD as well as MD exhibits history-dependence, as the contact forces at the end of the sample preparation and the yielding torque depend on g_{\max} . Secondly, only half of the funnel observed at lower angles operates as before.

One may ask how the CD simulation can exhibit memory, because it deduces the contact forces from the principles stated in Sec. II, but the history of the packing does not enter into those considerations. The memory of the CD algorithm comes from the way it chooses the contact forces. It begins with an initial guess, which it then refines through an iterative process until it arrives at a satisfactory solution. One usually takes the initial guess to be the solution of the previous time step because convergence is faster. But in Fig. 6, it is clear that this choice of initial guess also serves to make the CD algorithm history dependent, as the solution chosen depends on the initial guess [5]. But this memory is not the same as in the MD simulations. Nor is it clear why the preparation of the sample makes a difference at $\phi = 80^\circ$ but not at $\phi = 50^\circ$.

But the most important difference with the previous examples is that only half of the funnel works as before. As was noted earlier, there is no longer an upper bound on a_0 ; Eqs. (9a) and (9c) are both lower bounds. From the figure, one can see that the lower bound set by Eq. (9a) functions as before. When a_0 reaches this lower bound, it then increases linearly as the torque is increased, until equality is obtained in both Eqs. (9a) and (9c). Then the disk begins to rotate. The behavior of the lower bound set by Eq. (9c) is quite different. When equality is obtained in that condition, the value of a_0 jumps discontinuously, and the particle begins to rotate. As a result, the yielding torque is determined by when the system first satisfies equality in Eq. (9c), and this in turn depends on the value of a_0 set by the preparation phase of the experiment. Thus in this case, the memory does affect the yielding torque. In Sec. IV B, we will explain this discontinuity in a_0 theoretically. But one can already understand its physical origin. Equality in Eq. (9c) corresponds to contact β becoming sliding, meaning that tangential motion is now possible there. Since contact α is non-sliding, the particle pivots about contact α . As we showed earlier, contact β cannot open when $\tan \phi > \mu$, but the disk can apparently move enough to reduce the contact forces very quickly, allowing the particle to rotate.

In Fig. 7, we show the yielding torque as a function of g_{\max} . It is initially independent of g_{\max} , corresponding to the case where the system first meets the lower edge of the funnel. Then, CD and MD give different yielding torques. The MD values are well predicted by a result that will be obtained in Sec. IV B 3.

The CD values for the yielding torque are equal to or below the MD ones, because a_0 decreases as the torque is increased, while in the MD case, a_0 remains constant. This is plainly visible in Fig. 6. The different CD points correspond to different iteration procedures. The CD al-

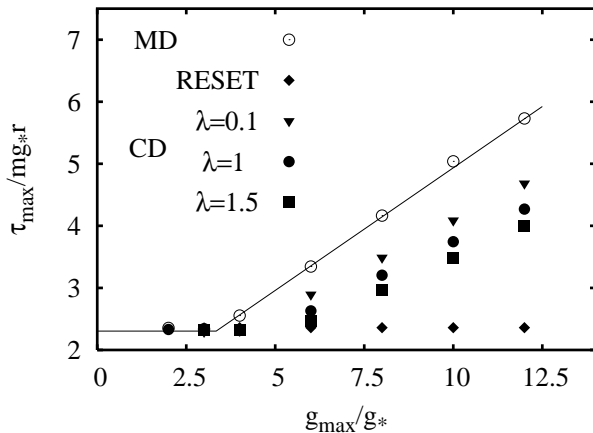


FIG. 7: The torque at which the disk begins to rotate at $\phi = 80^\circ$ and $\mu = 0.5$, for different values of g_{\max} . The four different sets of points for CD correspond to the different iteration algorithms described in the text. The line shows the theoretical prediction given in Sec. IV B 3.

gorithm searches for a solution by adjusting the contact forces one by one. It considers a given contact, and calculates the change in its contact forces needed to prevent interpenetration and minimize sliding. It then adds this to change to its current guess for the forces. After passing over all the contacts a certain number of times, the changes in the force needed fall below a certain threshold, and the solution is accepted. But this procedure can be altered by multiplying the calculated change in forces by a number λ , with $\lambda = 1$ corresponding to the usual iteration procedure. Changing λ changes the yielding torque, as shown above. Furthermore, the memory in the CD algorithm can be erased at each time step by always using $\mathbf{F} = 0$ as the initial guess, instead of the solution of the last time step. When this is done, one obtains the points labelled “RESET” in Fig. 7 and the yielding torque is independent of g_{\max} . This result emphasizes the important role of memory in this experiment.

IV. DEFORMABLE PARTICLES

A. Formalism

We now present a second method of calculating the contact forces that is able to explain all features of the MD simulations presented in the previous section. The cost of this additional information is that more assumptions must be made. First of all, one must specify how the forces depend on the deformations, but more significantly, one must specify the past history of the packing. This method shows how *indeterminacy* is replaced by *memory*. More precisely, when $\tan \phi > \mu$, we show that a_0 in Eq. (6) stores information about the largest downward force that has been exerted on the disk in the past.

Indeed, a_0 is a quantification of the “degree of wedging” discussed in Ref. [5].

We model the deformations in a very simple way, assuming that contact forces are generated by springs that are stretched by the motion of the disk. Our model is inspired by the MD simulation method [15], but we apply it analytically to our simple problem. A more general and realistic calculation has been presented before [13], but our purpose here is to show how the indeterminacy is replaced by history-dependence when forces arise from deformations.

When two bodies touch, a normal and a tangential spring be created at the instant of contact. The contact forces are simply proportional to the spring lengths:

$$R = -k\delta_n, \quad T = -k\delta_t, \quad (18)$$

where δ_n and δ_t are the normal and tangential spring lengths, and k is the spring constant. One normally includes damping in Eq. (18), but we will assume that the motion is quasi-static, i.e., a sequence of equilibrium states. Under this assumption, the particle velocities are vanishingly small, and so are the damping forces. However, the damping has important consequences that will be discussed below. Eq. (18) leads to a vector equation for \mathbf{F} in terms of the spring lengths \mathbf{D} :

$$\mathbf{F} = -k\mathbf{D}, \quad (19)$$

where $\delta_{n,\alpha}$, $\delta_{t,\alpha}$, $\delta_{n,\beta}$, and $\delta_{t,\beta}$ are gathered into \mathbf{D} just as the contact forces are arranged in \mathbf{F} [see Eq. (4)].

In general, one could introduce different spring constants for the normal and tangential springs, and the ratio of these spring constants affects the behavior of the system, even in the limit of infinitely hard particles. We set both spring constants equal, because it simplifies the results, and our purpose here is only to show how the indeterminacy is removed. But we remark that the ratio of the spring constants does not appear when the particles are rigid, indicating that the physics associated with this parameter has been eliminated.

The spring lengths obey

$$\dot{\delta}_n = v_n, \quad \dot{\delta}_t = \begin{cases} v_t, \\ \pm \mu v_n, \end{cases} \quad (20)$$

where v_n and v_t are the normal and tangential components of the relative velocity. There are two choices for $\dot{\delta}_t$ because $\mu R \geq |T|$ means that the tangential spring has a maximum allowable length: $|\delta_t| \leq \mu\delta_n$. If applying $\dot{\delta}_t = v_t$ would lead to a violation of this condition, the second choice is taken. Eq. (20) relates the time derivative of \mathbf{D} to the velocity of the disk. If all contacts are non-sliding, we have

$$\begin{aligned} \dot{\delta}_{n,\alpha} &= v_x \sin \phi + v_y \cos \phi, \\ \dot{\delta}_{t,\alpha} &= v_x \cos \phi - v_y \sin \phi + r\omega, \\ \dot{\delta}_{n,\beta} &= -v_x \sin \phi + v_y \sin \phi, \\ \dot{\delta}_{t,\beta} &= v_x \cos \phi + v_y \sin \phi + r\omega. \end{aligned} \quad (21)$$

Gathering the velocities of the disk into a single vector:

$$\mathbf{v} = \begin{pmatrix} v_x \\ v_y \\ \omega \end{pmatrix}, \quad (22)$$

Eqs. (21) becomes

$$\dot{\mathbf{D}} = \mathbf{c}^T \mathbf{v}, \quad (23)$$

where \mathbf{c}^T is the transpose of \mathbf{c} in Eq. (3). The appearance of \mathbf{c}^T is not a coincidence, but a general property valid for all granular packings [16].

It remains to incorporate the status of the contacts into our formalism. This can be done by inserting a matrix \mathbf{S} that depends on the contact status into Eq. (23):

$$\dot{\mathbf{D}} = \mathbf{S} \mathbf{c}^T \mathbf{v}, \quad (24)$$

where

$$\mathbf{S} = \begin{pmatrix} S_\alpha & 0 \\ 0 & S_\beta \end{pmatrix}. \quad (25)$$

Here, $S_\alpha = 1$ if contact α is non-sliding, $S_\alpha = 0$ if it is open, and

$$S_\alpha = \begin{pmatrix} 1 & 0 \\ \pm\mu & 0 \end{pmatrix}, \quad (26)$$

if it is sliding.

Finally, let us not forget Newton's equation of motion:

$$\mathbf{M} \dot{\mathbf{v}} = \mathbf{c} \mathbf{F} + \mathbf{f}_{\text{ext}}. \quad (27)$$

Here, the matrix \mathbf{M} contains the mass m and moment of inertia I of the disk on the diagonal:

$$\mathbf{M} = \begin{pmatrix} m & 0 & 0 \\ 0 & m & 0 \\ 0 & 0 & I \end{pmatrix}. \quad (28)$$

Eqs. (19), (24), and (27) form a set of equations that can be solved for the motion of the disk. Note that \mathbf{c} remains constant because all contacts are between the disk and the straight walls. The status of the contacts can change, however, so it is useful to divide time up into segments $[t_0, t_1], [t_1, t_2], \dots$, where the changes of contact status occur at the times t_1, t_2, \dots . In the interior of a time interval, the matrices \mathbf{c} , \mathbf{S} , and \mathbf{M} are constant, so Eqs. (19), (24), and (27) can be combined into

$$\mathbf{M} \ddot{\mathbf{v}} = -\mathbf{Q} \mathbf{v} + \dot{\mathbf{f}}_{\text{ext}}, \quad (29)$$

where $\mathbf{Q} = k \mathbf{c} \mathbf{S} \mathbf{c}^T$. The matrix \mathbf{Q} gives the change in force that arises from a small displacement of the disk. From this equation, the importance of the sign of $\mathbf{v}^T \mathbf{Q} \mathbf{v}$ can be seen. If $\mathbf{v}^T \mathbf{Q} \mathbf{v} > 0$, then \mathbf{Q} acts like a nonnegative number in Eq. (29), so that the contacts generate forces opposing the velocities \mathbf{v} , and hence \mathbf{v} will tend to

oscillate about an equilibrium value depending on $\dot{\mathbf{f}}_{\text{ext}}$. If the damping is chosen properly, these oscillations will be damped out very quickly, so \mathbf{v} will always be close to its equilibrium value. Physically, this means that \mathbf{v} is slaved to $\dot{\mathbf{f}}_{\text{ext}}$, as long as \mathbf{f}_{ext} changes much more slowly than the damping time scale. This amounts to removing the inertia from Eq. (29) and obtaining

$$\mathbf{Q} \mathbf{v} = \dot{\mathbf{f}}_{\text{ext}}. \quad (30)$$

The situation is different if \mathbf{f}_{ext} causes displacements that are in the null space of \mathbf{Q} , i.e., $\mathbf{v}^T \mathbf{Q} \mathbf{v} = 0$. In this case, no forces opposing the displacements are generated, and they can grow without bound, leading to permanent rearrangements of the particles. Another possibility is that $\mathbf{v}^T \mathbf{Q} \mathbf{v} < 0$. In this case, the contact forces amplify the velocities, which then grow exponentially. In this case, the packing fails catastrophically, with the contact forces changing much more quickly than \mathbf{f}_{ext} .

Finally, let us note there is a compatibility condition between \mathbf{S} and \mathbf{v} that must be satisfied: \mathbf{v} must be such that the tangential springs stay stretched to their maximum lengths. If this condition is not fulfilled at a contact, then that contact becomes non-sliding, and \mathbf{S} must be modified.

Let us now show how all this can be used to calculate the contact forces without indeterminacy. We will do so by calculating the coefficients of the expansion in Eq. (6). We can construct an equation for these coefficients by differentiating Eq. (19) with respect to time, and combining it with Eq. (24), leading to $\dot{\mathbf{F}} = \mathbf{S} \mathbf{c}^T \mathbf{v}$. Then we project this equation onto the basis given in Eq. (5) by left-multiplying it by \mathbf{a} , a 4×4 matrix whose rows are the basis vectors in Eq. (5), but without the factor of $1/2$. After doing this, we obtain

$$\begin{pmatrix} \dot{a}_x \\ \dot{a}_y \\ \dot{a}_\theta \\ \dot{a}_0 \end{pmatrix} = k \mathbf{a} \mathbf{S} \mathbf{c}^T \mathbf{v}. \quad (31)$$

Eq. (31) represents four equations, one corresponding to each of a_x , a_y , a_θ , and a_0 . The first three coefficients are known from Eq. (7), thus the first three equations above can be used to find the three components of \mathbf{v} . Then the last equation can be used to determine \dot{a}_0 . The displacement of the disk from its equilibrium position is obtained by integrating \mathbf{v} .

B. Application

1. Shallow angles: $\tan \phi < \mu$

When $\tan \phi < \mu$, the contacts remain non-sliding until the disk begins to rotate. Therefore, we can consider the entire experiment to take place during one time interval.

When the contacts are non-sliding,

$$k\mathbf{aSc}^T = 2k \begin{pmatrix} 1 & 0 & r \cos \phi \\ 0 & 1 & 0 \\ 0 & 0 & r \sin \phi \\ 0 & 0 & 0 \end{pmatrix}. \quad (32)$$

Using this result in Eq. (31), we have

$$\begin{aligned} \dot{a}_x &= 2kv_x + 2kr\omega \cos \phi, \\ \dot{a}_y &= 2kv_y, \\ \dot{a}_\theta &= 2kr\omega \sin \phi, \\ \dot{a}_0 &= 0. \end{aligned} \quad (33)$$

From the last line, we can see that a_0 remains constant as long as the contacts are non-sliding. This explains why $a_0 = 0$ for all the MD simulations in Fig. 4: $a_0 = 0$ at the beginning of the simulation, and thus remains so until the disk rolls. This also explains why a_0 is constant when g is decreases in Figs. 5 and 6.

Next let us calculate the disk's motion. Eqs. (33) can be solved for the velocities and integrated. In this way, the position \mathbf{r} of the disk can be shown to be

$$\mathbf{r} = \frac{1}{2k} \begin{pmatrix} 0 \\ -mg \\ \tau/(r^2 \sin^2 \phi) \end{pmatrix}. \quad (34)$$

Because no contact changes its status, the motion is perfectly reversible. This is another way to see that the packing has no memory when $\tan \phi < \mu$.

2. Intermediate slopes: $\mu < \tan \phi < 1/\mu$

When $\tan \phi > \mu$ and $t < t_A$, the contacts are sliding with $T_\alpha = -\mu R_\alpha$ and $T_\beta = \mu R_\beta$:

$$k\mathbf{aSc}^T = 2k \cos^2 \phi \begin{pmatrix} \tan^2 \phi - \mu \tan \phi & 0 & 0 \\ 0 & 1 + \mu \tan \phi & 0 \\ -\tan \phi - \mu \tan^2 \phi & 0 & 0 \\ 0 & \tan \phi - \mu & 0 \end{pmatrix}. \quad (35)$$

Changes in contact status will occur, so it is necessary to subdivide the experiment into time intervals. The first change of status occurs at $t = t_A$, when the derivative of the gravity changes sign, so we define our first interval to end at $t = t_A$. We can find the particle displacements using the same method as before, and find,

$$r_y(t_A) = -\frac{mg_{\max}}{2k} \frac{\sec^2 \phi}{1 + \mu \tan \phi}. \quad (36)$$

As before, $r_x(t_A) = r_\theta(t_A) = 0$. We also have $a_0(t_A) = a_{\text{mem}}$, with

$$a_{\text{mem}} = mg_{\max} \frac{\tan \phi - \mu}{1 + \mu \tan \phi}. \quad (37)$$

When the gravitational force begins to decrease, all contacts are non-sliding. The displacements must be calculated using the matrix given in Eq. (32). As before,

the particle rises by a distance $m(g_{\max} - g_*)/(2k)$, while a_0 remains unchanged. The particle's position is now

$$r_y = -\frac{mg_* + a_{\text{mem}}}{2k}. \quad (38)$$

It is important to realize that this is *not* the same as would have been obtained if the gravity was simply increased directly to g_* . This is another expression of the packing's memory, but it is much more convenient to think of the memory being located in a_0 . Eq. (38) mingles information about the past with information about the present, whereas Eq. (37) contains information only about the past. This is a consequence of using the basis in Eq. (5), where what is determined directly by the imposed forces is separated from what is not.

When the torque is applied, the contacts are still non-sliding, and they remain so until one of the contacts becomes sliding. We can determine which contact slides first by checking if a_{mem} is greater than or less than a_2 . If $a_{\text{mem}} < a_2$, then the system meets the lower side of the funnel first, meaning contact α slides. Otherwise, it meets the upper edge first, and contact β slides. Using Eqs. (17) and (37), we obtain that $a_{\text{mem}} > a_2$ is equivalent to

$$g_{\max} > g_* \left(1 + \frac{\mu}{\tan \phi} \frac{1 + \tan^2 \phi}{1 + \mu^2} \right). \quad (39)$$

If this condition holds, then as τ increases, a_0 decreases to maintain equality in Eq. (9c). Eventually, equality is obtained in Eq. (9a), i.e., contact α begins to slip as well, and the disk rotates. This occurs when $a_0 = a_2$, with a_2 given in Eq. (17). On the other hand, if Eq. (39) is not obeyed, then contact α slips first. Then a_0 increases until $a_0 = a_2$, and the disk begins to rotate. Evaluating Eq. (39) for $\mu = 0.5$, $\phi = 50^\circ$, one obtains $g_{\max} \approx 1.8g_*$, consistent with Fig. 5, where simulations with $g_{\max}/g = 2, 4, 6, 8$ all meet the upper edge of the funnel.

3. Steep slopes: $\tan \phi > 1/\mu$

For $\tan \phi > 1/\mu$, all the calculation in the previous section applies. The only difference is that the slope of the line given by equality in Eq. (9c) changes sign. This line is shown in Fig. 6, and if the system were to behave as before, it would follow this line upward indefinitely, leading to an infinite torque. However, the simulations show otherwise. When Eq. (9c) is attained, the system suddenly jumps to the rotating state, in a behavior qualitatively different from the other cases. This jump occurs when $T_\beta = -\mu R_\beta$, so this suggests that we ought to calculate the displacements of the disk in this situation. We calculate the matrix $k\mathbf{aSc}^T$ as before, and assume that the torque is increasing. Calculating the velocity of the disk \mathbf{v} in the usual way, one obtains

$$\mathbf{v} = \frac{\dot{\tau}}{2k(1 - \mu \tan \phi)} \begin{pmatrix} \mu - \tan \phi + \sec \phi \csc \phi \\ \tan \phi (\mu + \tan \phi) \\ \frac{1}{r} \sec^2 \phi \csc \phi \end{pmatrix}. \quad (40)$$

Note the factor $1 - \mu \tan \phi$ in the denominator, which is positive when $\tan \phi < 1/\mu$ and negative when $\tan \phi > 1/\mu$. Let us pause for a moment to consider what this change of sign means for ω . Applying a positive torque to the disk means trying to rotate it in the positive direction, i.e., trying to impose $\omega > 0$. When $\tan \phi < 1/\mu$, Eq. (40) shows that rotating the particle in this direction generates contact forces that balance an increasing torque. Therefore, the configuration is stable: when τ increases, the particle rotates in the positive direction, and the contact forces balance the increased torque. On the other hand, when $\tan \phi > 1/\mu$, the particle must be rotated in the *negative* direction to balance an increasing torque. But such a torque will always rotate the disk in the positive direction. Thus, the configuration is unstable. The small increase in torque causes the particle to rotate in the positive direction as before. But this rotation causes the forces opposing the torque to decrease, which in turn causes the particle to rotate farther in the positive direction. This leads to a rapid change in the contact forces as the particle begins to rotate. Another way to see this is to calculate $\mathbf{v}^T \mathbf{Q} \mathbf{v}$ using the value of \mathbf{v} given above. One obtains

$$\mathbf{v}^T \mathbf{Q} \mathbf{v} = \frac{\dot{\tau}^2}{2kr} \frac{\csc^2 \phi \sec^2 \phi}{1 - \mu \tan \phi}, \quad (41)$$

which becomes negative for $\tan \phi > 1/\mu$. Thus the particle interactions no longer oppose the applied force, but amplify it. This leads to an exponential growth of the motion, and the rapid change in the forces observed in the simulations.

We can now predict the yielding torque in the MD simulations. If Eq. (39) is not satisfied, the system meets the lower edge of the funnel that functions normally, and the disk rotates when $\tau = \tau_2$. An example of this is the MD simulation at $g_{\max}/g = 2$ in Fig. 6. On the other hand, if Eq. (39) is satisfied, the system meets the other branch of the funnel, and immediately starts to rotate. We can calculate the torque where this happens because the value of a_0 is known. Thus inserting the value of a_0 given in Eq. (37) into Eq. (9c) and solving for the torque gives

$$\tau = mr \sin \phi \left[g_* + g_{\max} \left(\frac{\tan \phi - \mu}{\tan \phi + \mu} \frac{\mu \tan \phi - 1}{\mu \tan \phi + 1} \right) \right]. \quad (42)$$

This result accurately predicts the yielding torque, as shown in Fig. 7.

V. CONCLUSIONS

We have carried out an intensive investigation of a very simple system. This has enabled us to precisely understand certain principles of the quasi-static motion of granular packings. First of all, there is the relation between memory and indeterminacy. When particles are

assumed to be rigid, the forces cannot be uniquely determined. A certain combination of forces, whose amplitude is given by the coefficient a_0 in Eq. (6), causes no acceleration, and thus cannot be deduced by examining the equations of static equilibrium. However, its value can be constrained by enforcing Coulomb friction and the absence of cohesion at all the contacts. On the other hand, when the particles are assumed to be deformable, a_0 contains information about the history of the packing. This finding suggests that methods that average over different possible force networks [2] are really averaging over past histories of the packing.

Secondly, we were able to precisely understand the connection between indeterminacy and motion. Depending on the angle ϕ , the onset of motion of the disk can take two different forms. When $\tan \phi < 1/\mu$, the range of allowed values of a_0 decreases continuously, and vanishes precisely at the onset of motion, and the torque needed to turn the disk is independent of method and history of the packing. Furthermore, the forces change slowly and continuously. A second mode of failure is more dramatic. When $\tan \phi > 1/\mu$, the indeterminacy is infinite, i.e., there is no upper bound on a_0 . At the onset of motion, the forces change discontinuously (on the time scale of changes in the imposed torque), and the torque needed to turn the disk depends on the history and method. This mode of failure is related to a curious situation in which the contact forces no longer oppose the applied forces, but enhance it.

This work shows that giving the CD iterative solver the the solution of the last time step as the initial guess is not just a numerical trick to accelerate convergence. It is an essential part of the method that represents a real physical process at work in granular material, namely the memory of the packing encoded in the combinations of force that cause no acceleration. In certain situations, this memory could have an important effect on the behavior of the packing.

It is hoped that the findings presented in this paper will deepen and clarify our understanding of the quasi-static deformation of much larger packings. When the number of particles is larger, there is not just one undetermined combination of forces, but many. However, one can expect that the effects studied here will be present in these more complicated situations, perhaps combined with each other in new and unexpected ways.

Acknowledgments

The authors want to acknowledge the EU project *Degradation and Instabilities in Geomaterials with Application to Hazard Mitigation* (DIGA) in the framework of the Human Potential Program, Research Training Networks (HPRN-CT-2002-00220). The authors wish to thank F. Alonso-Marroquín and J.J. Moreau for encouragement and interesting discussions.

-
- [1] F. Radjai, L. Brendel, and S. Roux, *Phys Rev E* **54** 861 (1996)
- [2] J.H. Snoeijer, T.J.H. Vlugt, M. van Hecke, and W. van Saarloos, *Phys. Rev. Lett.* **92** 054302 (2004).
- [3] T. Unger, J. Kertész, and D.E. Wolf, submitted to *Phys. Rev. Lett.*
- [4] S.McNamara and H.Herrmann, accepted by *Phys. Rev. E* (2004).
- [5] J.J. Moreau, *European Congress on Computational Methods in Applied Sciences and Engineering*, P. Neitaanmäki, T. Rossi, S. Korotov, E. Oñate, J. Périaux, and D. Knörzer, eds. (2004)
- [6] L. Vanel, D. Howell, D. Clark, R.P. Behringer, and Eric Clément, *Phys. Rev. E* **60** R5040 (1999).
- [7] H. Matuttis, S. Luding, and H. Herrmann, *Powder Technology* **109** 278 (2000).
- [8] J. Geng, E. Longhi, R.P. Behringer, and D.W. Howell, *Phys. Rev. E* **64** 060301 (2001).
- [9] M. Oda and H. Kazuma, *Géotechnique* **48** 465 (1998).
- [10] M. Oda and K. Iwashita, *Int. J. of Eng. Sci.* **38** 1713 (2000).
- [11] F. Alonso-Marroquín and H.J. Herrmann, *Phys Rev Lett* **92** 054301 (2004).
- [12] R. García-Rojo and H. Herrmann, accepted by *Granular Matter*.
- [13] T.C. Halsey and D. Ertas, *Phys. Rev. Lett.* **83** 5007 (1999).
- [14] J.J. Moreau, in *Novel Approaches in Civil Engineering*, M. Frémond and F. Maceri, eds, *Lecture Notes in Applied and Computational Mechanics* **14** 1 (2004).
- [15] P.A. Cundall and D.L. Strack, *Géotechnique* **29** 47 (1979).
- [16] J.-N. Roux, *Phys. Rev. E* **61** 6802 (2000).